Chapter 54
Magnetic Nanocomposite Sorbents on Mineral Base

Oksana Makarchuk, Tetiana Dontsova, and Anatolii Perekos

54.1 General

54.1.1 Introduction

Sorption purification is the most commonly used and suitable for adaptation to industrial conditions technology [1–3]. The high sorption capacity of sorbent minerals including clay minerals is provided by their colloidal dispersion. But in wastewater treatment process, the problem of removing spent sorbent particles from the aquatic environment is appeared.

Classical separation methods of sorbent sludge from purified water like centrifugation, filtration, upholding, coagulation, and flocculation processes are unacceptable in industrial-scale purification. Centrifugation is too energy intensive and, therefore, costly process. Filtration in this case is complicated from engineering and technological point of view due to the high dispersion of sorption material. Purification by upholding is a too long process. The destabilization of wastewater suspension by coagulation and flocculation processes requires the use of large number of different reagents. The cost of reagents calls into question the economic viability of this technology. In addition, none of these conventional methods can guarantee elimination of secondary water pollution risk [4].

O. Makarchuk (✉) • T. Dontsova
National Technical University of Ukraine "Kyiv Polytechnic Institute", Kyiv, Ukraine
e-mail: xtfhn9207@ukr.net; dontsova@ua.fm

A. Perekos
Institute of Magnetism of the NAS of Ukraine and Ministry for Education and Science of Ukraine, Kyiv, Ukraine
e-mail: perekos@ukr.net

O. Fesenko, L. Yatsenko (eds.), *Nanophysics, Nanomaterials, Interface Studies, and Applications*, Springer Proceedings in Physics 195,
DOI 10.1007/978-3-319-56422-7_54

In [5] the profitability of magnetic separation, process in wastewater filtering of the steel-making company was calculated. It was found that the removal of suspended particles from the water medium in the magnetic filter was 24 times faster compared to conventional filter with the same level of capital expenditures, operating costs, and occupied production area.

The process of magnetic separation can be realized in a magnetic field created by a permanent magnet or an electromagnet. In implementing purification technology in industrial level, an external magnetic field created by using permanent magnets is acceptable, because in this case, the magnetic field strength does not require constant electricity consumption [6, 7].

Magnetic separation process can be adapted to the adsorption technology of purification by [8]:

Direct adsorption of pollutants on magnetic particles
Introduction of a magnetic modifier as flocculant for magnetic particle coagulation of spent sorbent
Application of magnetic composite sorbents

Magnetic iron oxides are costly and not porous sorbents. The combination of processes of contaminants adsorption on magnetic particles, magnetic separation, and flocculation is a complex problem, which includes a significant number of manufacturing operations and requires the use of a large amount of equipment and production areas. Among these methods, the most technologically and economically favorable form of magnetic support of sorption treatment is the use of magnetic composite sorbents [9, 10].

Manageability of ferromagnetic particle deposition process in a magnetic field is determined not only by their size and magnetic characteristics but the magnetic nature of the matrix in which they are stabilized [11]. The clays are paramagnetic substances, and in magnetic separator, their mineral matrices are magnetized in the direction of the external magnetic field. Such feature of clays provides the decisive influence to choose them as a basis for magnetic composite sorbent creation [12].

This study shows the results of the physical, chemical, and magnetic properties of composite magnetic-controllable sorbents based on clays, and it presents an assessment of effectiveness to their use in magnetic field.

54.1.2 Materials and Methods

Magnetic composite sorbents were prepared by impregnation method. The natural saponite, palygorskite, and spondyle clays were sieved to the particle size less than 230 meshes (63 μm) and dispersed in magnetic fluid. The obtained mixture was mechanically stirred for 30 min in order to adsorb Fe_3O_4 on the surface and pores of clay. The synthesized sorbent was separated in magnetic filter at magnetic induction of external magnetic field of 66 mT and dried at 60–80 °C for 1 day.

Thus, samples of magnetic sorbents (MC) based on saponite (MCSp-4, MCSp-7, MCSp-10), palygorskite (MCP-4, MCP-7, MCP-10), and spondyle clays (MCSd-4, MCSd-7, MCSd-10) containing 4 wt.%, 7 wt.%, and 10 wt.% of magnetite were obtained.

Measurement of mass concentration of chemical elements in sample MC was carried by nondestructive energo-dispersive roentgen analysis method without standards using analyzer EXPERT 3 L.

Powder X-ray diffractions (XRD) of all sorbent samples were recorded using a Rigaku Ultima IV diffractometer using Cu Kα radiation at 40 KV, 30 mA. Orientated samples were scanned from 2° to 162° 2-theta at 1°/min with a scanning step of 0.0001°/step. Crystallographic Open Database (COD) was applied for phase composition definition of sorbents. The crystallite sizes and the unit cell parameters of magnetite and magnetite in magnetic composites were calculated with software package PDXL using the Scherrer's formula.

The morphologies of the synthesized products were observed using a scanning electron microscope (SEM 106 M).

Magnetic properties of nanocomposites (specific magnetization σ_S (A•m^2/kg); magnetic field strength H_c (A/m); magnetic induction B_r (mT)) were determined by ballistic magnetometer of Steinberg.

High-gradient magnetic separation of MC and native clays was studied in magnetic filter. Magnetic induction of external magnetic field was 66 mT. The residual concentrations of suspended sorbent particles in an aqueous medium through 5, 30, and 60 min of magnetic separation were determined by turbidimetry method.

54.2 Experimental

54.2.1 Chemical Analysis

Measurements of chemical composition in the sorbent samples were carried out by nondestructive energy-dispersive XRF analysis without standards and results listed in the Table 54.1 (MCSp and saponite clay), Table 54.2 (MCP and palygorskite clay), and Table 54.3 (MCSd and spondyle clay).

The results of elemental composition analysis of MC and natural clays showed the directly proportional growth of Fe concentration in depending on the increase of Fe_3O_4 content in composites at a relatively constant concentration of the basic elements of crystal clay lattice Mg, Al, Si, and Ca.

54.2.2 X-ray Analysis

Powder X-ray diffractions of magnetite, MC, and natural clays were recorded using a Rigaku Ultima IV diffractometer. The corresponding diffraction patterns are

Table 54.1 Chemical analysis of the composites MCSp and saponite clay

	Saponite	MCSp-4	MCSp-7	MCSp-10
Chemical element	Content, % wt.			
Mg	5.34–7.18	4.09–6.23	4.69–5.61	3.64–5.14
Al	4.90–5.76	3.77–4.97	1.19–2.15	1.57–2.33
Si	20.68–22.67	20.32–22.40	18.44–20.06	15.92–17.42
S	0.00–0.18	0.14–0.36	0.02–0.04	0.02–0.04
Ca	24.57–26.86	17.83–19.84	15.54–17.81	14.27–16.17
Ti	2.22–2.98	2.38–2.59	1.22–2.43	1.35–1.97
V	0.15–0.20	0.20–0.29	0.10–0.19	0.11–0.21
Mn	0.87–1.21	0.69–0.77	0.73–0.82	0.56–0.65
Fe	*35.94–37.35*	*45.30–47.17*	*52.75–55.47*	*57.28–60.71*
Ni	0.05–0.12	0.05–0.07	0.06–0.09	0.06–0.08
Cu	0.11–0.14	0.08–0.10	0.07–0.10	0.09–0.11
Zn	0.09–0.18	0.10–0.11	0.10–0.12	0.10–0.12
Sr	0.05–0.1	0.03–0.05	0.05–0.06	0.02–0.03

Table 54.2 Chemical analysis of the composites MCP and palygorskite clay

	Palygorskite	MCP-4	MCP-7	MCP-10
Chemical element	Content, % wt.			
Al	4.48–5.79	5.42–6.72	4.65–5.97	4.70–6.24
Si	52.22–55.12	42.69–45.51	43.48–45.42	41.83–44.02
S	0.20–0.50	0.15–0.20	0.05–0.09	0.07–0.15
Cl	2.36–3.37	0.37–1.59	0.84–1.05	0.52–1.14
Ca	6.56–8.75	6.07–7.93	2.58–4.97	2.42–3.72
Ti	1.79–2.03	1.13–1.56	0.72–0.99	0.63–1.26
Mn	0.15–0.22	0.20–0.26	0.19–0.26	0.11–0.15
Fe	*26.97–28.83*	*38.58–40.73*	*42.20–45.83*	*44.49–48.01*
Zn	0.07–0.09	0.08–0.10	0.06–0.08	0.07–0.09
Sr	0.08–0.11	0.11–0.13	0.06–0.09	0.06–0.07
Rb	0.02–0.04	0.04–0.05	0.03–0.04	0.02–0.03
Zr	0.05–0.06	0.08–0.10	0.09–0.11	0.04–0.05
Pb	0.05–0.08	0.09–0.12	0.06–0.09	0.05–0.07

presented in Fig. 54.1 (magnetite), Fig. 54.2 (MCSp and saponite clay), Fig. 54.3 (MCP and palygorskite clay), and Fig. 54.4 (MCSd and spondyle clay).

Diffraction pattern of magnetite (Fig. 54.1) demonstrated strong peaks at 30.72 °, 35.38 °, 43.72 °, 53.64 °, 57.24 °, and 62.86 ° 2-theta attributed to the Fe_3O_4 (card № 01–071-6336). No other impurities were observed. Hence, the method of Elmore allows obtaining the pure magnetic-modifying agent.

The XRD pattern of the native saponite (Fig. 54.2a) had indicated peaks that correspond to saponite (card № 00–013-0305), montmorillonite (card № 00–002-0014), quartz (card № 00–001-0649), and calcite (card № 00–002-0623). The crystal plane diffraction peaks of composite sorbent MCSp-4 (Fig. 54.2b), MCSp-7 (Fig. 54.2c), and MCSp-10 (Fig. 54.2d) detected the presence of inherent phases of native saponite clay and found peaks that corresponded to Fe_3O_4.

Table 54.3 Chemical analysis of the composites MCSd and spondyle clay

	Spondyle clay	MCSd-4	MCSd-7	MCSd-10
Chemical element	Content, % wt.			
Si	19.26–23.08	21.37–24.34	20.25–22.53	18.35–20.93
S	1.07–1.47	0.67–0.88	0.54–0.73	0.60–0.98
Cl	1.17–1.45	0.35–0.55	0.39–0.48	0.81–1.08
Ca	56.54–59.37	45.53–49.04	40.70–45.29	36.23–39.10
K	3.59–3.72	3.16–3.95	2.81–2.91	2.51–2.62
Ti	2.01–2.23	1.61–1.81	1.38–1.52	1.07–1.25
Fe	*11.05–13.32*	*21.92–23.97*	*28.57–31.12*	*35.15–38.70*
Zn	0.04–0.05	0.04–0.05	0.03–0.04	0.03–0.04
Sr	0.18–0.19	0.24–0.26	0.21–0.22	0.16–0.17
Rb	0.03–0.04	0.04–0.05	0.04–0.05	0.03–0.04
Zr	0.05–0.06	0.07–0.08	0.06–0.08	0.06–0.08
Pb	0.02–0.03	0.02–0.03	0.02–0.03	0.01–0.02

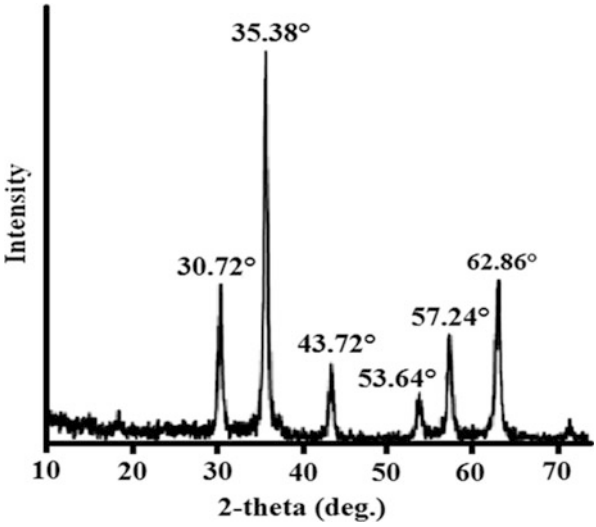

Fig. 54.1 The XRD patterns of magnetite Fe_3O_4

The XRD pattern of native palygorskite (Fig. 54.3a) consists of peaks that correspond to own palygorskite (card № 01–082-1872) and quartz (card № 00–001-0649). Diffraction patterns (Fig. 54.3b–d) confirmed the presence of magnetite in the presence of native clay phases in the composition of sorbents MCP-4, MCP-7, and MCP-10, respectively.

According to the X-ray diffraction analysis presented in Fig. 54.4a, spondyle clay consists of two minerals such as augite (card № 01–088-0831) and pigeonite (card № 01–087-0693). Phase composition of samples MCSd-4, MCSd-7, and MCSd-10 differs from native spondyle clays by the presence of magnetite peaks, which are identified in the Fig. 54.4b–d, respectively.

The X-ray analysis results of magnetic composites, native clay minerals, and magnetite phase confirmed stability of the mineral base and a magnetic modifier in the composition of obtained sorbents. As shown in the Figs. 54.2, 54.3, and 54.4,

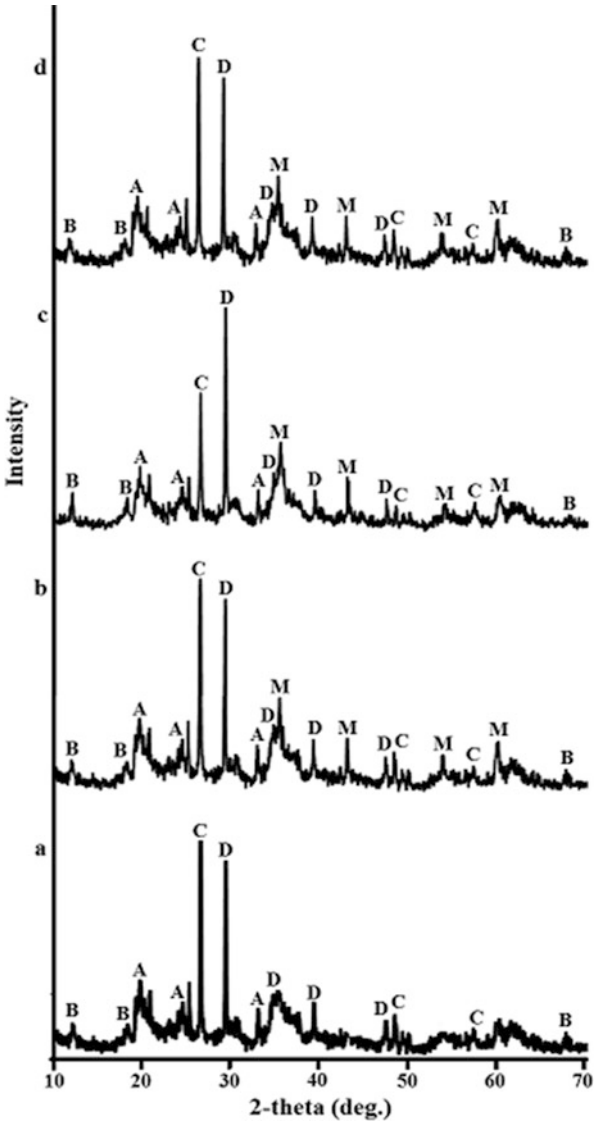

Fig. 54.2 The XRD patterns of saponite clay (**a**), MCSp-4 (**b**), MCSp-7 (**c**), and MCSp-10 (**d**): A, saponite $NaMg_3[AlSi_3O_{10}](OH)_2{\cdot}4H_2O$; B, montmorillonite $NaMgAlSiO_2(OH){\cdot}H_2O$; C, quartz SiO_2; D, calcite $CaCO_3$; M, magnetite Fe_3O_4

the increasing of peak intensity of magnetite is corresponded with increasing of magnetic modifier content in the MC samples from 4% wt. to 10 wt. Thus, as a result of composite synthesis, the phase composition of different natural sorption materials such as saponite, palygorskite, and spondyle clays was retained and supplemented by magnetic oxide Fe_3O_4.

The XRD patterns of MC and magnetite were automatically analyzed by software package PDXL using COD. The crystallite sizes and the unit cell parameters of

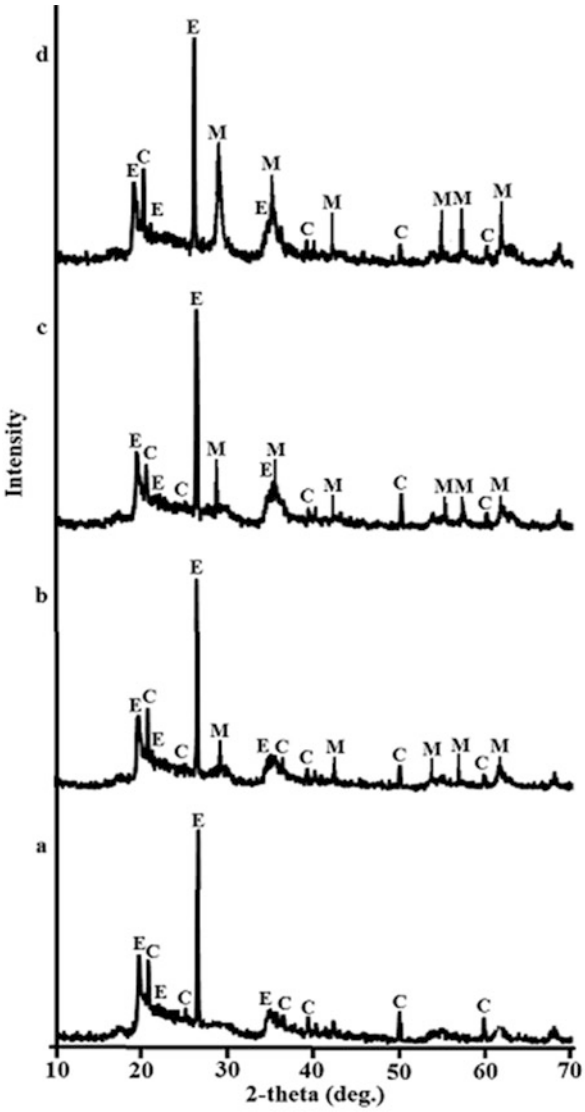

Fig. 54.3 The XRD patterns of palygorskite clay (**a**), MCP-4 (**b**), MCP-7 (**c**), and MCP-10 (**d**): E, palygorskite $(Mg_{0.669}, AI_{0.331})_4(Si_4O_{10})_2(OH)_2 \cdot 8H_2O$; C, quartz SiO_2; M, magnetite Fe_3O_4

magnetite and magnetite in magnetic composites were calculated and reported in Table 54.4.

As follows from the Table 54.4, magnetite in composite sorbents was obtained in the nanometer range. The average crystallite size of Fe_3O_4 nanoparticles was 5–10 nm.

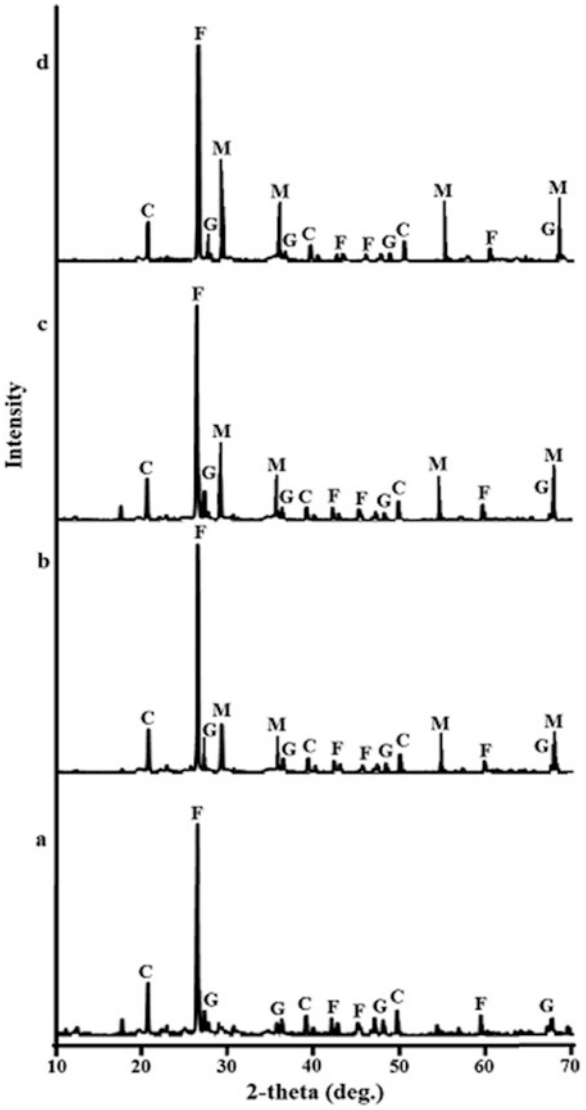

Fig. 54.4 The XRD patterns of spondyle clay (**a**), MCSd-4 (**b**), MCSd-7 (**c**), and MCSd-10 (**d**): F, augite Ca(Mg, Fe, Al) $[(Si, Al)_2O_6]$; G, pigeonite (Ca, Mg, Fe)(Mg, Fe)Si_2O_6; C, quartz SiO_2; M, magnetite Fe_3O_4

54.2.3 Microscopy

The SEM micrographs of saponite clay and MCSp (Fig. 54.5), palygorskite clay and MCP (Fig. 54.6), spondyle clay and MCSd (Fig. 54.7) were received and compared with an increase in 7850 times. These images show that magnetite had precipitated on the surface of clay minerals unequally. Tables 54.5, 54.6, and 54.7 present selective sorbent surface chemical analysis of the nanocomposites and natural clays.

Table 54.4 X-ray analysis of magnetic sorbents on the base of saponite, palygorskite, spondyle clays and magnetite

Sample	Average size of Fe_3O_4 crystallites, nm	Cell parameters, nm		
		a	b	c
MCSp-4	6.2	0.833	0.833	0.833
MCSp-7	9.6	0.833	0.833	0.833
MCSp-10	7.4	0.838	0.838	0.838
MCP-4	5.0	0.848	0.848	0.848
MCP-7	2.5	0.844	0.844	0.844
MCP-10	5.8	0.837	0.837	0.837
MCSd-4	4.9	0.856	0.856	0.856
MCSd-7	9.2	0.831	0.831	0.831
MCSd-10	10.3	0.836	0.836	0.836
Fe_3O_4	17.9	0.835	0.835	0.835

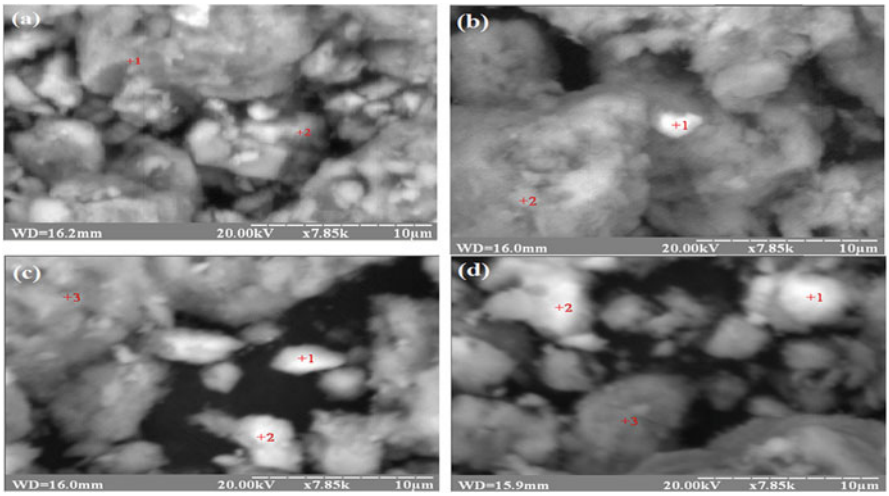

Fig. 54.5 SEM images of samples surfaces: saponite clay (**a**), MCSp-4 (**b**), MCSp-7 (**c**), and MCSp-10 (**d**)

As can be seen from the data, Fe content on the surface of clay matrix is increased with increasing amounts of magnetite in the structure of composites.

54.2.4 Magnetic Characteristics

The specific saturation magnetization, coercive force, and magnetic induction of saponite, palygorskite, and spondyle clays, Fe_3O_4, and synthesized MC samples are reported in the Table 54.8. Natural clays were characterized by specific saturation

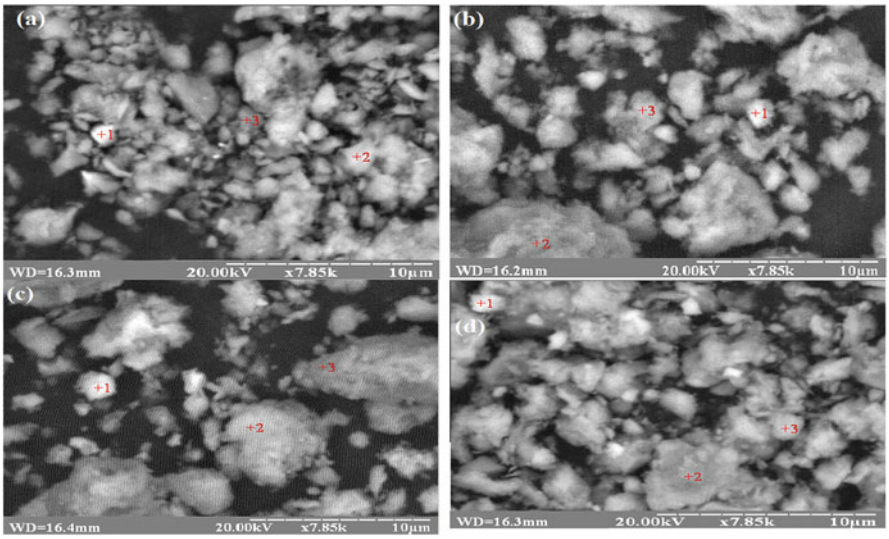

Fig. 54.6 SEM images of samples surfaces: palygorskite clay (**a**), MCP-4 (**b**), MCP-7 (**c**), and MCP-10 (**d**)

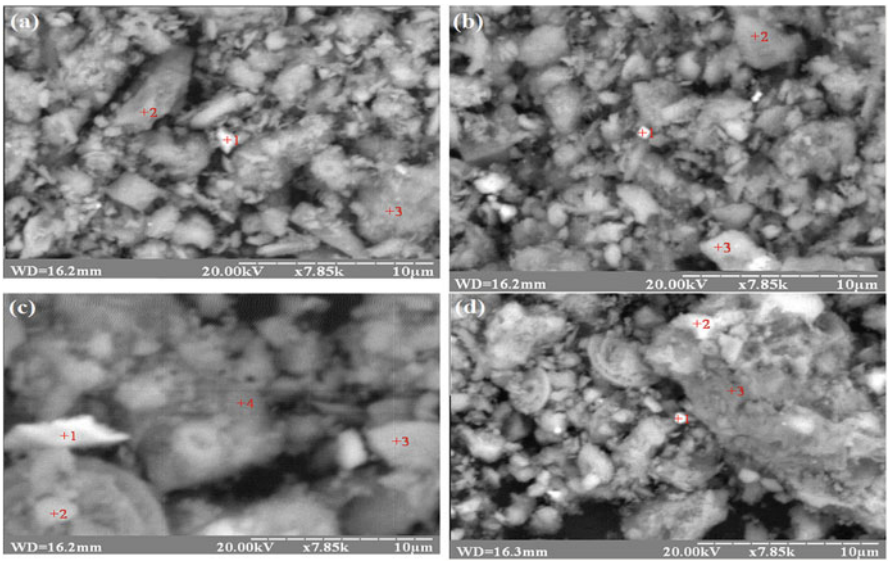

Fig. 54.7 SEM images of samples surfaces: spondyle clay (**a**), MCSd-4 (**b**), MCSd-7 (**c**), and MCSd-10 (**d**)

Table 54.5 Results of point chemical analysis of the saponite clay and nanocomposites MCSp

Chemical element	Contents, %			
Point	1	2	1	2
Sample	Saponite clay		MCSp-4	
Mg	8.52	6.3	1.8	5.7
Al	15.25	13.42	1.9	12.8
Si	39.4	40.43	6.2	36.8
Ca	4.88	5.6	1.7	3.4
Fe	31.95	34.25	88.4	41.3
Sample	MCSp-7		MCSp-10	
Mg	0.4	2.7	1.1	0.4
Al	0.7	3.0	1.6	0.7
Si	2.5	9.8	6.2	2.2
Ca	4.2	7.6	0.8	0.3
Fe	92.2	76.9	90.3	96.4

Table 54.6 Results of point chemical analysis of the palygorskite clay and nanocomposites MCP

Chemical element	Contents, %			
Point	1	2	1	2
Sample	Palygorskite clay		MCP-4	
Mg	0.96	0.87	1.03	1.85
Al	11.9	9.89	8.79	11.48
Si	69.31	77.96	50.68	61.39
Ca	2.39	2.09	1.44	2.34
Fe	15.44	9.19	38.06	22.94
Sample	MCP-7		MCP-10	
Mg	0.19	1.73	0.67	0.17
Al	0.39	13.04	6.62	4.7
Si	4.56	57.82	44.39	25.16
Ca	0.41	3.34	2.21	1.31
Fe	94.45	24.07	46.11	68.66

Table 54.7 Results of point chemical analysis of the spondyle clay and nanocomposites MCSd

Chemical element	Contents, %			
Point	1	2	1	2
Sample	Spondyle clay		MCSd-4	
Mg	4.26	5.72	0.43	0.37
Al	1.68	3.93	3.67	4.93
Si	16.89	15.54	19.59	17.54
Ca	71.12	68.96	36.19	48.96
Fe	6.05	5.85	40.12	28.2
Sample	MCSd-7		MCSd-10	
Mg	0.2	0.53	0.01	0.16
Al	1.43	2.4	0.84	1.38
Si	5.24	9.87	2.96	4.91
Ca	42.65	12.44	40.52	5.32
Fe	50.48	73.9	55.67	88.23

Table 54.8 Magnetic characteristics of sorbent samples

Sample	$\sigma_{S(10)}$, A•m^2/kg	H_c, A/m	B_r, mT
Saponite clay	0	0	0
MCSp-4	3.0	0	0
MCSp-7	4.5	954.9	1.20
MCSp-10	6.5	954.9	1.10
Palygorskite clay	0	0	0
MCP-4	3.0	636.6	0.16
MCP-7	3.9	954.9	0.10
MCP-10	7.3	3819.7	0.57
Spondyle clay	0	0	0
MCSd-4	2.0	795.8	0.09
MCSd-7	6.3	1909.9	0.20
MCSd-10	8.3	2864.8	0.57
Fe_3O_4	90.0	501.3	3.50

zero magnetization; therefore, these minerals were classified as paramagnetic materials. When paramagnetic mineral matrix of composite modified by nanomagnetite enters to the magnetic separator, it is magnetized in the direction of the external magnetic field. So, controllability of magnetic separation process is determined by the properties of modifier ferromagnetic particles.

Most popular magnetic modifiers, such as magnetite Fe_3O_4 and maghemite γ-Fe_2O_3, in the nanoscale state showed specific behavior in a magnetic field compared to monolithic magnetic materials [13]. Nanoscale magnetic modifier is characterized by super paramagnetic properties and low residual magnetization (soft magnetic materials). As is known [14], the magnetite change of reversal mechanism from reorientation of magnetic moments (single-domain state) to displacement of domain walls (poly-domain state) for magnetite occurred when the size of nanoparticles approximately 30 nm.

In the synthesis of MCSp, MCP, and MCSd in the clay matrix, the Fe_3O_4 crystallites were formed about the same size of 2–10 nm (Table 54.4). Based on this, the specific saturation magnetization of MC samples was gradually increased with growing of magnetite content. Hence, the nanoscale magnetite particles of MC were formed with the same magnetization and arrangement of spins in one direction.

For MC samples containing magnetite in an amount of less than 7%wt., coercive force Hc and residual magnetic induction Br are characterized by significantly lower values. Size of Fe_3O_4 nanoparticles in the composition of these samples is smaller than 5 nm. For single-domain magnetic particles, there is some critical value of size in which the coercive force disappears, and they become superparamagnetic state. In the case of Fe_3O_4, this critical diameter corresponds to 5–6 nm. In a superparamagnetic state, magnetite nanoparticles behave like substance consisting of very small ferromagnetic particles, weakly interacting with each other.

Table 54.9 The magnetic separation process of saponite, palygorskite, and spondyle clays and nanocomposites MCSp, MCP, and MCSd

Sample	C, mg/dm^3		
	5 min	30 min	60 min
Saponite clay	558.8	387.7	327.1
MCSp-4	121.6	17.7	14.3
MCSp-7	32.7	1.0	<0.5
MCSp-10	16.6	<0.5	<0.5
Palygorskite clay	662.7	418.2	351.6
MCP-4	186.6	69.3	21.6
MCP-7	26.6	<0.5	<0.5
MCP-10	24.3	<0.5	<0.5
Spondyle clay	713.8	526.0	464.9
MCSd-4	126.6	37.1	23.8
MCSd-7	14.9	5.4	<0.5
MCSd-10	9.9	<0.5	<0.5

Magnetization of nanoparticles is easy for operating since it is determined by the ordering of atoms of magnetic structure [15]. Thus, magnetic particles of magnetite in the nanometer range have specific superparamagnetic properties, and MC samples belong to the soft magnetic materials. It is worth mentioning that nanosized iron oxide particles over time can aggregate and form hard magnetic materials with high value of residual magnetization. The use of hard magnetic materials complicates the regeneration of magnetic separator.

Fe_3O_4 is introduced into the larger particles (clay matrix) for practical application in the process of magnetic separation. This is caused by the large hydrodynamic resistance and the tendency of nanoscale magnetic particles to aggregate. The interaction of magnetic nanoparticles with an applied magnetic field provides the controlled deposition of magnetic composite which dispersion can vary depending on the requirements of water purification technology [16, 17].

54.2.5 Magnetic Separation

Table 54.9 shows the kinetics of separation of clay minerals and magnetic composites based on them. Separation of magnetic sorbents from the purified solution in a filter equipped with permanent magnets was held in 36 times faster.

The 98% of spent magnetic sorbent mass were precipitated for the first 5 min of magnetic separation, and purified water was suitable for discharge into the centralized sewage. Application of magnetic composites has ensured the achievement of the residual concentration of suspended solids $\leq$0.02 mg/L for 30 min of magnetic separation.

54.3 Conclusions

Magnetic composite sorbents on mineral base (saponite, palygorskite, and spondyle clays) were created by impregnation method. The pure magnetic-modifying agent Fe_3O_4 was obtained by method of Elmore.

In the synthesis of MCSp, MCP, and MCSd in the clay matrix, the Fe_3O_4 crystallites were formed approximately in the same range (5–10 nm). The specific saturation magnetization of MC samples was approximately the same which agrees with crystallite sizes. Magnetic particles of magnetite in the nanometer range were characterized by specific superparamagnetic properties, and MC were classified to the soft magnetic materials.

The removal of spent magnetic sorbents occurred almost three times faster compared to native clay, and the residual concentration of suspended solids in the water corresponded to standards for drinking water (<0,5 mg/dm^3). Thus, practical effectiveness magnetic separation method for the deposition of spent sorbents from the water was confirmed.

Acknowledgments The authors thank the G.V. Kurdyumov Institute for Metal Physics, National Academy of Sciences of Ukraine, for their support in conducting this research.

References

1. Mortazavi S, Farmany A (2016) High adsorption capacity of MWCNTs for removal of anionic surfactant SDBS from aqueous solutions. J Water Supply Res Technol 65:160–166
2. Gan F, Luo Y, Hang X, Zhao H (2016) Heterocoagulated clay-derived adsorbents for phosphate decontamination from aqueous solution. J Environ Manage 166:23–30
3. Elmoubarki R, Mahjoubg FZ, Tounsadj H et al (2015) Adsorption of textile dyes on raw and decanted Moroccan clays: kinetics, equilibrium and thermodynamics. Water Resou Ind 9:16–29
4. Wang LK, Hung Y, Lo H (2006) T Waste treatment in the Process Industries. Taylor & Francis Group, Boca Raton, pp 307–453
5. Yavuz CT, Prakash A, Mayo JT, Colvin VL et al (2009) Magnetic separations: from steel plants to biotechnology. Chem Eng Sci 64:2510–2521
6. Zhu ZQ, Howe D (2001) Halbach permanent magnet machines and applications: a review. Proc on Electr Power Appl 148(4):299–308
7. Li XL, Yao KL, Liu HR, Liu ZL (2007) The investigation of capture behaviors of different shape magnetic sources in the high-gradient magnetic field. J Magn Magn Mater 311(2):481–488
8. Ambashta RD, Sillanpaa M (2010) Water purification using magnetic assistance: a review. J Hazard Mater 180:38–49
9. Mykhailenko NO, Makarchuk OV, Dontsova TA et al (2015) Purification of aqueous media by magnetically operated saponite sorbents. East Eur J Enterp Technol 10(76):13–20
10. Makarchuk OV, Dontsova TA, Astrelin IM (2015) Magnetic clay sorbent for the removal of dyes from aqueous solutions. Research bulletin of the National Technical University of Ukraine "Kyiv Polytechnic Institute" 6, p 109–114
11. Makarchuk OV, Dontsova TA, Astrelin IM (2016) Magnetic nanocomposites as efficient sorption materials for removing dyes from aqueous solutions. Nanoscale Res Lett 161(11):1–7

12. Galindo-Gonzalez C, Vicente J, Ramos-Tejada MM et al (2005) Preparation and sedimentation behavior in magnetic fields of magnetite-covered clay particles. Langmuir 21(10):4410–4419
13. Sun J, Xu R, Zhang Y, Ma M, Gu N (2007) Magnetic nanoparticles separation based on nanostructures. J Magn Magn Mater 312(2):354–358
14. Doroshenko A, Chekman I (2014) Magnetic nanoparticles: properties and biomedical applications. Ukrainian Med J 4(102):10–13
15. Clime L, Drogoff BL, Zhao S et al (2008) Magnetic nanocarriers: from material design to magnetic manipulation. Int J Nanotechnol 5(9):1268–1305
16. Latham AH, Williams ME (2008) Controlling transport and chemical functionality of magnetic nanoparticles. Acc Chem Res 41(3):411–420
17. Pathak A, Panda AB, Tarafdar A et al (2003) Synthesis of nano-sized metal oxide powders and their application in separation technology. J Indian Chem Soc 80(4):289–296